

NASA TECHNICAL NOTE



NASA TN D-8280

NASA TN D-8280

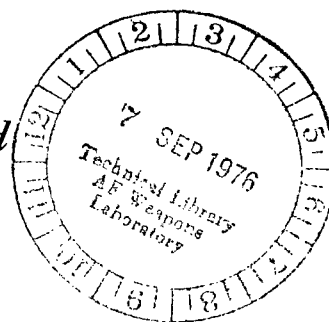
LOAN COPY:  
AFWL TECHNICAL  
KIRTLAND AFB



MICROSTRUCTURAL CHANGES CAUSED  
BY THERMAL TREATMENT AND THEIR  
EFFECTS ON MECHANICAL PROPERTIES  
OF A  $\gamma/\gamma'$  -  $\delta$  EUTECTIC ALLOY

*Surendra N. Tewari and Robert L. Dreshfield*

*Lewis Research Center  
Cleveland, Ohio 44135*





0133998

|  |  |   |
|--|--|---|
| 1. Report No.<br>NASA TN D-8280  | 2. Government Accession No.  | 3. Recipient's Catalog No.                              |
| 4. Title and Subtitle<br>MICROSTRUCTURAL CHANGES CAUSED BY THERMAL TREATMENT AND THEIR EFFECTS ON MECHANICAL PROPERTIES OF A $\gamma/\gamma'$ - $\delta$ EUTECTIC ALLOY  | 5. Report Date<br>August 1976  | 6. Performing Organization Code                         |
| 7. Author(s)<br>Surendra N. Tewari and Robert L. Dreshfield  | 8. Performing Organization Report No.<br>E-8531                            | 10. Work Unit No.<br>505-01                             |
| 9. Performing Organization Name and Address<br>Lewis Research Center<br>National Aeronautics and Space Administration<br>Cleveland, Ohio 44135   | 11. Contract or Grant No.  | 13. Type of Report and Period Covered<br>Technical Note |
| 12. Sponsoring Agency Name and Address<br>National Aeronautics and Space Administration<br>Washington, D.C. 20546  | 14. Sponsoring Agency Code   |   |
| 15. Supplementary Notes  |  |   |
| 16. Abstract<br>Microstructural changes due to thermal treatments of a directionally solidified $\gamma/\gamma'$ - $\delta$ eutectic alloy were investigated. Aging treatments of 8 to 48 hours and ranging from 750 <sup>0</sup> to 1120 <sup>0</sup> C were given to the alloy in both its as directionally solidified condition and after $\gamma'$ solutioning. Aging resulted in $\gamma'$ coarsening, $\gamma$ precipitates in $\delta$ , and $\delta$ and $\gamma''$ precipitates in $\gamma$ . The tensile strength was increased about 12 percent at temperatures up to 900 <sup>0</sup> C by a heat treatment. Times to rupture were essentially the same or greater than for as directionally solidified material. Tensile and rupture ductility in the growth direction of the alloy were reduced by the heat treatment. |  |   |
| 17. Key Words (Suggested by Author(s))<br>Superalloys; Heat treatment; Eutectic;<br>Directional solidification   | 18. Distribution Statement<br>Unclassified - unlimited<br>STAR Category 26 |   |
| 19. Security Classif. (of this report)<br>Unclassified   | 20. Security Classif. (of this page)<br>Unclassified                       | 21. No. of Pages<br>35                                  |
|  |  | 22. Price*<br>\$4.00                                    |

# MICROSTRUCTURAL CHANGES CAUSED BY THERMAL TREATMENT AND THEIR EFFECTS ON MECHANICAL PROPERTIES OF A $\gamma/\gamma' - \delta$ EUTECTIC ALLOY\*

by Surendra N. Tewari<sup>†</sup> and Robert L. Dreshfield

Lewis Research Center

## SUMMARY

The purpose of this research was to study the microstructural changes due to thermal treatments of the directionally solidified (DS)  $\gamma/\gamma' - \delta$  eutectic alloy of the nominal composition nickel - 20 percent columbium - 6 percent chromium - 2.5 percent aluminum (by weight) and to select a heat treatment to provide improved tensile and stress-rupture properties. Microstructural changes were studied which resulted from aging treatments ranging from 8 to 48 hours at temperatures from 750<sup>o</sup> to 1120<sup>o</sup> C given to the alloy in both its as-DS condition and after a 4 hour at 1225<sup>o</sup> C complete  $\gamma'$  solutioning treatment.

The DS  $\gamma/\gamma' - \delta$  eutectic alloy consists of alternate lamellae of  $\gamma$  nickel solid solution with  $\gamma'$  Ni<sub>3</sub>Al precipitates and  $\delta$  Ni<sub>3</sub>Cb phase. Low temperature (750<sup>o</sup> and 800<sup>o</sup> C) aging resulted in only slight  $\gamma'$  coarsening. Intermediate temperature (900<sup>o</sup> and 950<sup>o</sup> C) aging resulted in  $\gamma'$  coarsening,  $\gamma$  precipitates in  $\delta$ , and  $\delta$  and  $\gamma''$  precipitates in  $\gamma$ . Elevated temperature (1040<sup>o</sup> and 1120<sup>o</sup> C) aging resulted in coarsened spheroidal  $\gamma'$  particles in  $\gamma$ .

Intermediate (24 hr at 900<sup>o</sup> C) and high temperature (8 hr at 1100<sup>o</sup> C) aging treatments were given to the as-DS, completely  $\gamma'$  solutioned, and partially  $\gamma'$  solutioned (4 hr at 1210<sup>o</sup> C) alloys. Tensile (925<sup>o</sup> C) and stress-rupture (870<sup>o</sup> C and 515 MN/m<sup>2</sup>) tests were conducted to select the best heat treatment condition for further study.

The selected heat treatment consisted of a partial  $\gamma'$  solution treatment followed by aging for 24 hours at 900<sup>o</sup> C. For temperatures below 900<sup>o</sup> C the heat-treated material had a tensile strength about 12 percent greater than as-DS material and for temperatures above 900<sup>o</sup> C its strength was the same as as-DS material. The stress-rupture life of the heat-treated alloy was essentially the same (870<sup>o</sup> and 1040<sup>o</sup> C) or greater (760<sup>o</sup> and 800<sup>o</sup> C) than for as-DS material. The tensile and rupture ductility in the growth direction for the heat-treated material tended to be lower than as-DS material.

---

\* Presented in part at the Annual Meeting of the American Institute of Mining, Metallurgical, and Petroleum Engineers, Las Vegas, Nevada, February 22-26, 1976, and the International Gas Turbine Conference sponsored by the American Society of Mechanical Engineers, New Orleans, Louisiana, March 21-25, 1976.

<sup>†</sup> National Research Council Associate.

## INTRODUCTION

Directionally solidified (DS) eutectics are likely to be the next generation material for gas turbine blades. Their use is expected to result in significant engine performance advantages due to a 50<sup>o</sup> to 100<sup>o</sup> C increase in allowable metal temperature over superalloys. This, in turn, could result in reduced fuel consumption and engine weight. One such eutectic is in the nickel-columbium-chromium-aluminum ( $\gamma/\gamma' - \delta$ ) system. Its microstructure consists of alternate lamellae of  $\gamma$  nickel solid solution with  $\gamma'$  Ni<sub>3</sub>Al precipitates and  $\delta$  Ni<sub>3</sub>Cb phase.

Significant changes in mechanical properties of superalloys have previously been obtained through the knowledge of structure-property relations resulting from empirical thermal treatments. One such study of a limited nature on a  $\gamma/\gamma' - \delta$  alloy has recently been reported (ref. 1). The purpose of this research was a larger effort to study the microstructural changes due to thermal treatments of an alloy within the  $\gamma/\gamma' - \delta$  system (nickel - 20 wt % columbium - 6 wt % chromium - 2.5 wt % aluminum, Ni-20Cb-6Cr-2.5Al) and to select a heat treatment to provide improved tensile and stress-rupture properties.

Aging treatments at several temperatures were given to the alloy in both its DS condition and after  $\gamma'$  solution treatment. The resulting microstructural changes were investigated by light and electron optics. A heat treatment condition was selected which provided a combination of improved high temperature tensile strength and stress-rupture life. Temperature dependence of tensile and stress-rupture properties was investigated for the selected thermal treatment condition.

## PROCEDURE

### Materials

Some 8 centimeter long by 1.3 centimeter diameter bars of the DS  $\gamma/\gamma' - \delta$  eutectic alloy of a nominal composition (Ni-20Cb-6Cr-2.5Al) were obtained from Pratt and Whitney Aircraft. These were grown at 3 or 4 centimeters per hour in a Bridgeman furnace having a temperature gradient in excess of 200<sup>o</sup> C per centimeter (ref. 2). Unreported work from this laboratory has shown no difference in tensile or stress rupture properties for this alloy grown at 3 and 4 centimeters per hour.

## Heat Treatments

Complete and partial  $\gamma'$  solutioning treatments given to the DS eutectic alloy consisted of 4-hour anneals in argon at 1225<sup>o</sup> and 1210<sup>o</sup> C, respectively, followed by an air quench. Aging treatments in low (750<sup>o</sup>, 800<sup>o</sup>, and 850<sup>o</sup> C), intermediate (900<sup>o</sup> and 950<sup>o</sup> C), and elevated (1040<sup>o</sup> and 1120<sup>o</sup> C) temperature ranges given to both as-DS and  $\gamma'$  solutioned eutectic alloy specimens in flowing argon for several aging times are compiled in table I. The microstructural changes due to these aging treatments were studied. Aging anneals of 24 hours at 900<sup>o</sup> C and 8 hours at 1100<sup>o</sup> C were given to the DS, completely  $\gamma'$  solutioned, and partially  $\gamma'$  solutioned eutectic alloy bars. These bars were used to select the heat treatment condition which had the best combination of high temperature tensile strength and stress-rupture life (table II). Material subjected to the selected heat treatment, 24 hours aging at 900<sup>o</sup> C of the partially solutioned eutectic alloy, was used to investigate the temperature dependence of tensile and stress-rupture properties.

## Mechanical Testing

Tensile tests and constant-load stress-rupture tests were conducted in air on the specimens using practices recommended by the American Society for Testing Materials (ASTM). Heat-treated bars were ground to the specimen dimensions shown in figure 1. Figure 1(a) shows the tapered-head specimens which were used for all the tensile tests and the initial stress-rupture tests. Very poor rupture life reproducibility was observed by Gray and Sanders (ref. 3) for DS  $\gamma/\gamma' - \delta$  eutectic alloy tapered-head specimens, especially for temperatures between 675<sup>o</sup> and 870<sup>o</sup> C. They further observed that by using threaded-head specimens this effect was greatly reduced. Therefore, temperature dependence of the stress-rupture properties of the heat-treated eutectic alloy was investigated by using the threaded-head specimens shown in figure 1(b). All tests were loaded parallel to the alloy growth direction.

## Metallography

Specimens were polished using normal metallographic procedures with a final polish of 0.5-micrometer alumina powder on microcloth. Specimens were etched by immersing 5 seconds in a solution of 30 cubic centimeters nitric acid, 30 cubic centimeters water, 30 cubic centimeters acetic acid, and 1 cubic centimeter hydrofluoric acid. Scanning electron microscopy was occasionally used to obtain higher magnifications.

For examination by replica transmission electron microscopy, specimens polished by the previous technique were etched electrolytically at 12 volts using a solution of 40 cubic centimeters lactic acid, 20 cubic centimeters saturated boric acid, 20 cubic centimeters citric acid (10 percent), and 20 cubic centimeters ammonium per sulfate (10 percent). Some specimens were ion etched with argon ions. Carbon replicas of the etched specimens were prepared by the conventional two-stage replication technique for examination by electron microscope.

Thin foils and minor phase extraction were used for identifying various precipitates by transmission electron microscopy and electron diffraction techniques. The procedures for thin foil preparation and minor phase extraction together with the observations on which the phase identifications are based are described in appendixes A, B, and C.

## RESULTS AND DISCUSSION

### Microstructural Changes Due to Thermal Treatments

The heat treatments investigated and a summary of the microstructural observations for as-DS and completely  $\gamma'$  solutioned alloys are listed in table I.

As-cast baseline condition. - Figure 2 shows the microstructure of the DS eutectic alloy. Figure 2(a), a transverse section (perpendicular to the alloy growth direction), shows that the eutectic alloy consists of alternate lamellae of  $\gamma$ , nickel solid solution with  $\gamma'$   $\text{Ni}_3\text{Al}$  precipitates, and  $\delta$   $\text{Ni}_3\text{Cb}$  (orthorhombic) phase. The alloy selected for this study was not perfectly lamellar (about 15 to 20 percent cellular). The cellular  $\delta$  and  $\gamma/\gamma'$  regions surrounded by lamellar regions can be observed in this figure. Occasionally some Widmanstätten type precipitates were observed in cellular  $\gamma/\gamma'$  regions (fig. 2(b)). These Widmanstätten precipitates in DS  $\gamma/\gamma' - \delta$  alloy were identified as  $\delta$  by bright and dark field image contrasts using thin foil transmission electron microscopy (appendix A). These are similar to the precipitates observed and identified as  $\delta$  in Ni- $\text{Ni}_3\text{Cb}$  DS eutectic by Annarumma and Turpin (ref. 4). The  $\gamma$  phase occasionally contained fine disk shaped precipitates decorating the cubical planes of  $\gamma$  (fig. 2(c)). These precipitates were chemically extracted and identified as  $\gamma''$ , body centered tetragonal  $\text{Ni}_3\text{Cb}$ , by transmission electron diffraction (appendix B). These precipitates appear very similar to the  $\gamma''$  precipitates observed in nickel base superalloy 718 (ref. 5). The cuboidal  $\gamma'$  particles in as-DS  $\gamma/\gamma' - \delta$  eutectic alloy averaged 0.4 micrometer on edge (fig. 2(c)).

$\gamma'$  solutioning conditions. - The extent of  $\gamma'$  solutioning as a function of annealing temperature was investigated to establish the  $\gamma'$  solutioning treatment. The previously reported value of  $\gamma'$  solutioning temperature, 1200<sup>o</sup> C (ref. 1), resulted in incomplete solutioning of  $\gamma'$ . Primary  $\gamma'$  which had not gone into solution was present after 4-hour

anneals at 1210<sup>o</sup> and 1220<sup>o</sup> C (figs. 3(a) and (b)). However, the 1230<sup>o</sup> C anneal resulted in complete solutioning of  $\gamma'$  (fig. 3(c)). On the basis of this microstructural observation, a 4-hour anneal in flowing argon at 1225<sup>o</sup> C followed by air quench to room temperature was selected as the complete  $\gamma'$  solutioning treatment. A replica electron micrograph shows the microstructure obtained after such a treatment (fig. 3(d)). This treatment did not produce any structural degradation of the  $\gamma/\delta$  interface even though the melting point of this alloy is only about 20<sup>o</sup> C higher than the  $\gamma'$  solutioning temperature. The exposure at 1225<sup>o</sup> C resulted in complete  $\gamma'$  solutioning; however, during air quenching, cuboidal  $\gamma'$  particles with an average size of 0.15 micrometer precipitated (fig. 3(d)). This is to be expected because of the extremely fast  $\gamma'$  nucleation and precipitation kinetics which is well known for superalloys (ref. 6). No  $\gamma''$  or Widmanstätten  $\delta$  precipitates were observed in the  $\gamma'$  solutioned alloy.

A 4-hour anneal in flowing argon at 1210<sup>o</sup> C followed by an air quench to room temperature was used for partial  $\gamma'$  solutioning treatments. As expected, this treatment resulted in a bimodal  $\gamma'$  size distribution consisting of coarse  $\gamma'$  particles which did not dissolve and fine  $\gamma'$  particles which precipitated during the air quench. The following sections describe the effect of several aging treatments on microstructures of the alloy both as-DS and as completely  $\gamma'$  solutioned. It should be noted, however, that these treatments applied to partially  $\gamma'$  solutioned material produced similar microstructures except for the bimodal  $\gamma'$  precipitate distribution in the partially solutioned material.

Low temperature aging treatments. - Aging treatments of the  $\gamma'$  solutioned eutectic alloy at 750<sup>o</sup> and 800<sup>o</sup> C alloy did not result in any significant microstructural change. At 850<sup>o</sup> C, however,  $\gamma''$  appeared to be precipitating in  $\gamma$  (fig. 4(a)). In this figure the preferential etching of  $\gamma/\gamma'$  near the  $\gamma/\delta$  interface is probably due to the chemistry changes associated with the interdiffusion of various elements between the lamellae. This preferential etching was more pronounced in the immediate vicinity of cellular regions and was not observed for a similar aging of as-DS alloy (fig. 4(b)).

For the previously mentioned 750<sup>o</sup>, 800<sup>o</sup>, and 850<sup>o</sup> C aging studies no microstructural change was observed, except slight  $\gamma'$  coarsening, in the as-DS alloy (fig. 4(b)). Both the  $\gamma''$  and Widmanstätten  $\delta$  precipitates shown in figure 4(b) were not due to the heat treatment and were present in the as-DS alloy (see fig. 2). This figure demonstrates the difference between the disk-like  $\gamma''$  and lath-like  $\delta$  precipitates. The  $\gamma''$  precipitates decorate the cubical planes of  $\gamma$  (ref. 5) and therefore appear in directions which are perpendicular to each other. Lath-like precipitates on the other hand decorate octahedral planes of  $\gamma$  (ref. 4).

Intermediate temperature aging. - Aging at 900<sup>o</sup> C of the completely  $\gamma'$  solutioned eutectic alloy increased the cuboidal  $\gamma'$  from about 0.15 to about 0.3 micrometer. Aging also resulted in thin needle-like precipitates decorating three equivalent planes in  $\delta$  (fig. 5(a)). Figures 5(b) and (c) show these precipitates at higher magnifications for

transverse and longitudinal (parallel to the alloy growth direction) sections, respectively. The long dimension of these precipitates is parallel to  $\gamma/\delta$  interface ( $100_{\delta}$  direction, ref. 2). Precipitates identified as  $\gamma'$  have previously been observed during the heat treatment of  $\gamma' - \delta$  DS eutectic alloy (ref. 7). However, due to the absence of superlattice diffraction spots in this investigation, these precipitates were assumed to be  $\gamma$  (appendix C). This aging treatment also resulted in Widmanstätten  $\delta$  precipitates appearing in  $\gamma$  (fig. 5(d)).

It is significant that both  $\gamma$  precipitates in  $\delta$  and  $\delta$  precipitates in  $\gamma$  occur more abundantly in cellular regions (fig. 5(a)). This is expected since cellular regions are the first to solidify; hence, they may be richer in solutes. The  $\gamma''$  particles in  $\gamma$  can also be observed in figure 5(d), which is a replica electron micrograph of the specimen which was aged at  $900^{\circ}\text{C}$  after a complete  $\gamma'$  solutioning treatment.

Similar precipitation of  $\gamma$  in  $\delta$  and  $\delta$  in  $\gamma$  was also observed in the as-DS specimens when aged at  $900^{\circ}\text{C}$  for 8 to 24 hours, though to a lesser degree than the  $\gamma'$  solutioned specimens (compare figs. 5(a) and (e)).

It can also be noted in figure 5(d) that in the immediate vicinity of  $\delta$  precipitates in  $\gamma$  the  $\gamma'$  particles (in the  $\gamma/\gamma'$  region) are more spheroidal than the ones which are further away from  $\delta$ . This observation is more clearly demonstrated in figure 6(a). The shape of  $\gamma'$  is believed to depend on the lattice mismatch between  $\gamma'$  and the matrix. Since  $\delta$  precipitation results in localized columbium depletion and columbium normally is partitioned to  $\gamma'$ , the  $\gamma'$  in the vicinity of Widmanstätten  $\delta$  would have a low columbium content. We suggest that this chemistry change is responsible for altering the local lattice mismatch between the  $\gamma'$  and the matrix in the vicinity of  $\delta$  precipitates.

The microstructure resulting from the aging treatment at  $950^{\circ}\text{C}$  (fig. 6) was not significantly different from that at  $900^{\circ}\text{C}$ . The  $950^{\circ}\text{C}$  aging yielded coarser  $\gamma'$  particles ( $0.29$  and  $0.38\ \mu\text{m}$  for 8- and 24-hr anneal, respectively); there were more Widmanstätten  $\delta$  precipitates in  $\gamma$  and less  $\gamma$  precipitates in  $\delta$  compared to the aging at  $900^{\circ}\text{C}$  (compare figs. 5(a) and 6(b)). The  $\gamma''$  precipitates can also be observed in as-DS specimens annealed at  $950^{\circ}\text{C}$ .

Elevated temperature aging. - Effects of elevated temperature ( $1040^{\circ}$  and  $1120^{\circ}\text{C}$ ) aging after the  $\gamma'$  solutioning treatment are shown in figure 7. The microstructure observed when a  $\gamma'$  solutioned specimen was annealed for 8 hours at  $1040^{\circ}\text{C}$  is shown in figure 7(a). The  $\gamma'$  particles were much coarser ( $0.48\ \mu\text{m}$ ) due to intermediate temperature aging, and they were spheroidal (fig. 7(b)) rather than cuboidal in shape. No  $\gamma''$  precipitates were observed in  $\gamma$ ; thus, the  $\gamma''$  solutioning temperature is between  $950^{\circ}$  and  $1040^{\circ}\text{C}$ . A similar microstructure was observed in as-DS specimens after an 8-hour anneal at  $1040^{\circ}\text{C}$ .

The microstructure for an 8-hour aging treatment at  $1120^{\circ}\text{C}$  following the  $\gamma'$  solutioning treatment (fig. 7(c)) shows that while the Widmanstätten  $\delta$  precipitates in  $\gamma$



were more numerous and coarser than at 1040<sup>o</sup> C the  $\gamma$  precipitates in  $\delta$  were less numerous and coarser than those for the aging treatment at 1040<sup>o</sup> C. The  $\gamma'$  particles in  $\gamma$  were quite large (0.68  $\mu\text{m}$ ) and spheroidal (fig. 7(d)). The precipitates in  $\delta$  are very similar to  $\gamma'$ ; however, no electron diffraction studies could be made of them because these precipitates were very few in number and seldom appeared in the thin foil TEM specimens prepared. In the absence of any definite proof and because of the similarity of their appearance to precipitates analyzed before (appendix C), these were assumed to be  $\gamma$  precipitates.

### Effect of Heat Treatments on Mechanical Properties

Heat treatment selection. - Based on the microstructural observations due to the various heat treatments shown in table I it was decided to evaluate the effect of aging at 900<sup>o</sup> and 1100<sup>o</sup> C on stress rupture life at 870<sup>o</sup> C and 515 meganewtons per square meter and tensile strength at 925<sup>o</sup> C. The 925<sup>o</sup> C temperature was selected because it was previously shown to be a temperature having low ductility (ref. 3). The lower aging temperature was selected because 900<sup>o</sup> C was the lowest temperature where significant  $\gamma'$  coarsening and  $\gamma$  precipitates in  $\delta$  were observed. The higher temperature, 1100<sup>o</sup> C, was selected to represent an overaging condition and to be indicative of temperatures achieved in potential coating cycles.

Three material conditions, as-DS, fully solution treated 4 hours at 1225<sup>o</sup> C, and partial solution treated for 4 hours at 1210<sup>o</sup> C, were selected for aging. The as-DS and solution treated at 1225<sup>o</sup> C conditions were selected as the limiting extreme conditions. The partial solution was thought to be more indicative of a practical maximum temperature, being only about 20<sup>o</sup> C below the reported solidus temperature.

Photomicrographs of the DS eutectic alloy which was partially solution treated and aged are shown in figure 8. Comparing figures 8(a) and (b) shows that aging even for shorter times at 1100<sup>o</sup> C produces a coarser  $\gamma'$  than does 900<sup>o</sup> C aging. The bimodal  $\gamma'$  size distribution resulting from the partial solution treatment is more apparent in figure 8(b). It was common in this investigation to see  $\gamma'$  dissolve at lower temperatures in the cellular regions than in the lamellar regions shown in figure 8(b). This phenomenon is presumed to occur because the cellular regions are the first to solidify and therefore would have different concentrations of solutes than the lamellar regions have. In this case, it is believed that an increase in chromium concentration is locally lowering the solvus temperature.

The effect of the heat treatments on the 925<sup>o</sup> C tensile strength (table II) is shown in figure 9(a). The strength varied from 800 meganewtons per square meter for the partial solution plus 1100<sup>o</sup> C age condition to 960 meganewtons per square meter for the full solution condition without aging. The solution treated and partial solution treated



materials were stronger than the as-DS material for both unaged specimens and those aged at 900° C. The average strength for material (both aged and unaged) after solution and partial solution treatment was 892 meganewtons per square meter; for material aged directly after growth the strength was 875 meganewtons per square meter. Material aged at 1100° C had an average strength of 833 meganewtons per square meter, which was lower than the average strength of 903 meganewtons per square meter for either 900° C aged or unaged material. The tensile elongation varied from 2 to 5 percent, but no correlation with the heat treatment condition was noted.

The effect of heat treatment on the 970° C and 515 meganewtons per square meter rupture life (table II) is shown in figure 9(b). The most apparent point is that aging increased the rupture life. The average life of aged material was 292 hours, while the average life of unaged material was only 112 hours. The longest rupture lives were observed for partially solutioned and aged material. It also appears that aging at 1100° C gave slightly greater rupture lives than aging at 900° C. The average life after 1100° C aging was 304 hours compared to 281 hours for material aged at 900° C. Rupture elongation varied from 6 to 10 percent, but it could not be correlated with heat treatment effects.

The microstructural feature which appears to influence the tensile strength is the  $\gamma'$  size. The higher temperature aging treatments result in larger  $\gamma'$  sizes presumably causing lower strengths. The fracture modes did not appear to change with heat treatment. A typical elevated temperature tensile fracture is shown in figure 10. The fracture is primarily trans-granular with some shearing of grain boundaries parallel to the growth direction. Secondary cracking appears to form first in  $\delta$  lamellae along twins. Cooperative twinning and deformation in  $\gamma$  and  $\delta$  lamellae result in kinking in the lamellar structure. The kinking is assumed to be a precursor to cracking and fracture. Portions of the fractured surface are therefore seen to be parallel to the twin directions and kinking direction in the alloy.

Based on the tensile and stress rupture results shown in figure 9, material which had been partially solution treated at 1210° C followed by aging 24 hours at 900° C was selected for further evaluation of tensile and stress rupture strengths. The selected heat treatment appeared to offer the best balance of tensile strength and rupture life of the nine conditions screened.

Effect of selected heat treatment on mechanical properties. - The tensile strength of  $\gamma/\gamma' - \delta$  which was partially solutioned at 1210° C and aged 24 hours at 900° C is listed in table III and compared to as-DS material (ref. 3) in figure 11. At temperatures somewhat below 1040° C the heat-treated material is about 12 percent stronger than the as-DS alloy. The average tensile strength of the heat-treated material decreased from 1405 meganewtons per square meter at room temperature to 980 meganewtons per square meter at 925° C. At 1040° C the alloy had a tensile strength of about 650 meganewtons per square meter for both the heat-treated and as-DS conditions.

At room temperature and 760<sup>o</sup> C the elongation of the heat-treated eutectic was about 50 percent lower than for the as-DS alloy. At 925<sup>o</sup> and 1040<sup>o</sup> C the elongation was essentially the same for both the heat-treated and as-DS alloy. It appears that for temperatures below the aging temperature of 900<sup>o</sup> C the heat treatment is beneficial to strength but adversely affects tensile elongation.

Duplicate stress rupture tests were run at temperatures from 760<sup>o</sup> to 1040<sup>o</sup> C at stresses from 760 to 150 meganewtons per square meter. The results of these tests are listed in table III and are shown on a Larson-Miller plot in figure 12. Also shown in figure 12 is a curve of the average results of threaded head test-bar tests of as-DS alloy (private communication with H. R. Gray of Lewis Research Center). The stress rupture strength of the heat-treated alloy can be seen to be similar to that of the as-DS material. Except for a single short life data point of 318.5 hours at 800<sup>o</sup> C, the life of the heat-treated alloy is greater than that of the as-DS alloy at temperatures of 760<sup>o</sup> and 800<sup>o</sup> C (table III). A rupture ductility of 1 percent was observed at 760<sup>o</sup> C and 760 meganewtons per square meter as compared to a range from 4 to 9 percent observed by Gray (of Lewis Research Center) for as-DS material. However, at temperatures above 760<sup>o</sup> C the rupture ductilities of the heat-treated alloy were essentially the same as the as-DS alloy.

This work has shown that modest improvements in tensile strength up to the aging temperature and perhaps of rupture life up to 800<sup>o</sup> C can be achieved in  $\gamma/\gamma' - \delta$  by applying a simple heat treatment. Heat treatment investigated by Lemkey et al. (ref. 1), 4 hours at 1200<sup>o</sup> C plus 40 hours at 871<sup>o</sup> C, resulted in about a 10 percent strength improvement at room temperature. However, the strength improvement rapidly vanished with increasing temperature and the heat-treated alloy showed lower strength than as-DS material at temperatures higher than 600<sup>o</sup> C. In addition, the strengths measured in this investigation are even greater than those reported for the same alloy grown at about twice the solidification rate used in this investigation (ref. 8). We suggest that the improvement in strength is related to the finer  $\gamma'$  size achieved by heat treating. The reasons for the apparent differences in mechanical properties between the partial and full solution treated materials are not understood.

Work by others on this alloy system has noted low shear strength parallel to the lamellar growth direction (ref. 9) and poor transverse ductility and rupture strength (private communication with K. D. Sheffler, Pratt and Whitney Aircraft, E. Hartford, Conn.). Because the most significant microstructural change noted in this investigation appears to be  $\gamma'$  size distribution and because crack propagation for off-axis loading has been shown to be along cell walls and grain boundaries (ref. 9), it is not expected that the heat treatments in this investigation should influence off-axis properties. However, an examination of our data in the light of work described in reference 3 suggests a promise of improved off-axis properties. Gray and Sanders observed large stress rupture data scatter between 675<sup>o</sup> and 870<sup>o</sup> C when they used tapered heat test specimens. We believe that this data scatter was caused by off-axis loading created by alinement

problems associated with their test configuration. In figure 9(b), where we used the tapered-head test configuration, the poorest life for an aged sample was almost twice the life of the best unaged sample for the 870° C and 515 meganewtons per square meter test conditions. For the same test conditions of 870° C and 515 meganewtons per square meter, it can be seen that the aged alloy has essentially the same life as Gray and Sanders observed for as-DS material where both investigations used threaded-head specimens (fig. 12). Also note that the rupture life of 350 hours obtained for the 870° C and 515 meganewtons per square meter test conditions with tapered head specimens is essentially the same as that obtained with threaded head specimens (table III(b) and fig. 12) for the alloy subjected to the selected heat treatment (4 hr at 1210° C followed by aging 24 hr at 900° C). One then concludes that the aged material for temperatures greater than 800° C is not significantly different from unaged alloy when both are tested with good axial alinement.

The reason for the apparent improved properties observed for aged material in our screening studies still needs attention. We suggest that the aging treatments (fig. 9(b)) in fact may reduce the sensitivity of the alloy to off-axis loading and thereby cause the aged material to appear better than the unaged material in stress rupture tests using the tapered head specimen. Perhaps the transverse ductility is improved. The effect of the selected heat treatment on transverse ductility was investigated by Pratt and Whitney Aircraft as part of a NASA funded program under contract Nas 3-17811. Use of the selected heat treatment approximately doubled (0.34 to 0.58 percent elongation) the transverse ductility of fully lamellar  $\gamma/\gamma' - \delta$  alloy (private communication with K. D. Sheffler, Pratt and Whitney Aircraft Company).

## SUMMARY OF RESULTS

The directionally solidified (DS)  $\gamma/\gamma' - \delta$  eutectic alloy had a nominal composition (in wt %) of Ni-20Cb-6Cr-2.5Al. The alloy was studied in both its DS condition and after  $\gamma'$  solutioning treatments. Intermediate and high temperature aging treatments were given to the directionally solidified, completely  $\gamma'$  solutioned, and partially  $\gamma'$  solutioned alloy, and stress rupture and tensile tests were conducted to select a heat treatment condition for further study. Temperature dependence of stress rupture and tensile properties was investigated to determine the effect of the selected heat treatment. The following results were obtained from this study:

1. The DS  $\gamma/\gamma' - \delta$  alloy consisted of alternate lamellae of  $\gamma$  nickel solid solution with cuboidal  $\gamma'$  Ni<sub>3</sub>Al precipitates and  $\delta$  Ni<sub>3</sub>Cb (orthorhombic). It was about 15 to 20 percent cellular. The  $\gamma$  phase contained fine disk shaped  $\gamma''$  (body centered tetragonal Ni<sub>3</sub>Cb) precipitates. Occasionally lath-like Widmanstätten  $\delta$  precipitates were observed in cellular  $\gamma/\gamma'$ .

2. Low temperature aging treatments for 16 and 48 hours at 750<sup>o</sup> and 800<sup>o</sup> C following complete  $\gamma'$  solutioning treatment (4 hr at 1225<sup>o</sup> C) did not result in any significant microstructural change, except slight  $\gamma'$  coarsening. After 850<sup>o</sup> C, however,  $\gamma''$  precipitates were observed in  $\gamma$ .

3. Intermediate temperature aging for 8 and 24 hours at 900<sup>o</sup> and 950<sup>o</sup> C following complete  $\gamma'$  solutioning treatment resulted in needle-like precipitates, identified as  $\gamma$ , decorating three equivalent planes in  $\delta$  and lath-like Widmanstätten  $\delta$  precipitates in  $\gamma$ . Both the  $\delta$  precipitates in  $\gamma$  and  $\gamma$  precipitates in  $\delta$  occurred much more abundantly in the cellular regions. Coarsened cuboidal  $\gamma'$  and disk-like  $\gamma''$  precipitates were also observed. However, aging at 950<sup>o</sup> C produced fewer and coarser  $\gamma$  precipitates in  $\delta$  than 900<sup>o</sup> C aging. Microstructural changes observed due to aging of as-DS alloy were similar to the ones due to aging after  $\gamma'$  solutioning treatments. Similar but fewer precipitates of  $\gamma$  in  $\delta$  and of  $\delta$  in  $\gamma$  were observed, and again the cellular regions were the preferred precipitation sites.

4. Elevated temperature aging at 1040<sup>o</sup> and 1120<sup>o</sup> C after a complete  $\gamma'$  solutioning treatment resulted in coarsened spheroidal  $\gamma'$  particles in  $\gamma$ . No  $\gamma''$  precipitates were observed in  $\gamma$ , suggesting that the  $\gamma''$  solutioning temperature lies between 950<sup>o</sup> and 1040<sup>o</sup> C. More and coarser  $\delta$  precipitates in  $\gamma$  and fewer and coarser  $\gamma$  precipitates in  $\delta$  were observed as the aging temperature was increased from 950<sup>o</sup> to 1040<sup>o</sup> C and then to 1120<sup>o</sup> C.

5. The best combination of 925<sup>o</sup> C tensile and 870<sup>o</sup> C stress rupture properties resulted from a heat treatment consisting of a partial  $\gamma'$  solution treatment of 4 hours at 1210<sup>o</sup> C followed by aging 24 hours at 900<sup>o</sup> C. For temperatures below 900<sup>o</sup> C the heat-treated material was about 12 percent stronger than as-DS material. The tensile strength resulting from this heat treatment varied from 1405 meganewtons per square meter at room temperature to 650 meganewtons per square meter at 1040<sup>o</sup> C. At 760<sup>o</sup> and 800<sup>o</sup> C the heat-treated alloy appears to have a greater stress-rupture strength than does the as-DS material. For temperatures from 870<sup>o</sup> to 1040<sup>o</sup> C the stress rupture strengths of heat-treated and as-DS material appear to be equivalent. The tensile ductilities in the growth direction were about 50 percent of those reported for as-DS material. The rupture ductilities were essentially the same as the as-DS material except for 760<sup>o</sup> C and 760 meganewtons per square meter where the ductility observed was 1 percent as compared to the 4 to 9 percent reported for the as-DS alloy.

6. Aging at 900<sup>o</sup> and 1100<sup>o</sup> C appeared to increase the rupture life at 870<sup>o</sup> C and 515 meganewtons per square meter for taper head specimens. It is postulated that this apparent improvement may be indicative of improvements in the transverse properties of the alloy.

Lewis Research Center,  
National Aeronautics and Space Administration,  
Cleveland, Ohio, April 9, 1976,  
505-01.

## APPENDIX A

### IDENTIFICATION OF $\delta$

Small disks (0.25-cm diam) were electric discharge machined from thin transverse slices (0.02 cm thick) obtained from the DS  $\gamma/\gamma' - \delta$  eutectic alloy. The disks were thinned down to about a 50-micrometer thickness by hand grinding on systematically advancing from 220 grit to 600 grit papers. Jet electropolishing technique with two jets, one from either side of the disk, was used to obtain the electron microscopy thin foils. The electropolishing was done at 0<sup>o</sup> C, 20 volts, and 64 milliamperes in a solution consisting of 500 cubic centimeters methanol, 20 cubic centimeters nitric acid, 50 cubic centimeters sulfuric acid, 50 cubic centimeters acetic acid, and 6 cubic centimeters hydrofluoric acid.

A bright field electron micrograph showing lath like precipitates in a  $\gamma/\gamma'$  region is shown in figure 13(a). A typical electron diffraction pattern obtained from the  $\gamma/\gamma'$  region containing these precipitates is shown in figure 13(b). The diffraction spots were identified based on the  $\gamma/\gamma' - \delta$  diffraction pattern analyzed by Lemkey et al. (ref. 2). It contains several  $\delta$  spots (enclosed in squares) besides the expected  $\gamma/\gamma'$  spots (enclosed in circles and designated with indices in parentheses) suggesting these precipitates to be  $\delta$  as has previously been observed in  $\gamma/\delta$  DS eutectic alloy (ref. 4). The  $002_{\delta}$  diffraction point was used to obtain a dark field image of the region shown in figure 13(a). The dark field electron micrograph (fig. 13(c)) shows the  $\delta$  region with one set of lath-like precipitates in adjacent  $\gamma/\gamma'$  in contrast simultaneously, thus demonstrating these lath-like precipitates to be  $\delta$ .

## APPENDIX B

### IDENTIFICATION OF $\gamma''$

A transverse section of the DS  $\gamma/\gamma' - \delta$  eutectic alloy mounted in Bakelite was metallographically polished, the final polish being 0.5 micrometer alumina powder on microcloth. It was etched for 5 seconds in a solution of 30 cubic centimeters glycerine, 30 cubic centimeters boric acid, 20 cubic centimeters ammonium bisulfate (10 percent), and 20 cubic centimeters citric acid (10 percent). A carbon film of about  $2.5 \times 10^{-8}$  meter (250 Å) thickness was deposited on the etched specimen surface in a vacuum evaporator. The coated surface was scribed lightly into 3-millimeter squares. The disk-shaped particles were extracted by using first an ice-cooled solution of ethanol - sulfuric acid (8:1) for undercutting the carbon film followed by electropolishing in a solution consisting of 465 cubic centimeters ethyl alcohol, 50 cubic centimeters acetic acid, 50 cubic centimeters sulfuric acid, 20 cubic centimeters nitric acid, and 6 cubic centimeters hydrofluoric acid at 25 volts and 30 milliamperes. Finally, the small squares of carbon extraction replicas were floated in water and captured on 300 mesh copper grids for examination in the electron microscope.

Figure 14 shows the fine disk-shaped precipitates extracted in the manner just outlined. The electron diffraction pattern obtained from these precipitates is shown in figure 14(b). Many of these spots were too faint to reproduce in figure 14(b). The microscope camera constant (k) was determined from measurements on a ring pattern obtained from an evaporated gold film. The interplaner spacings (d) for the extracted particles calculated from figure 14(b) are compiled in table IV. This table also lists the calculated values of interplaner spacings for various plane indices (hkl) of  $\gamma''$  ( $\text{Ni}_3\text{Cb}$  body centered tetragonal structure with  $a_0 = 3.6 \times 10^{-10}$  meter (3.624 Å) and  $c_0 = 7.4 \times 10^{-10}$  meter (7.406 Å); ref. 5). A good correlation between the observed and calculated d values can be observed in table IV demonstrating these precipitates to be  $\gamma''$ .



## APPENDIX C

### IDENTIFICATION OF $\gamma$ PRECIPITATES

A transverse section of the DS  $\gamma/\gamma' - \delta$  eutectic alloy specimen which had been  $\gamma'$  solutioned (4 hr at 1225<sup>o</sup> C) and aged for 8 hours at 900<sup>o</sup> C (table I) was examined by transmission electron microscopy to identify the fine precipitates observed in  $\delta$  (fig. 5). The same thin foil preparation technique described in appendix A was used.

Figure 15, a bright field electron micrograph, shows the fine precipitates in a  $\delta$  region. The electron diffraction pattern obtained from the region containing these precipitates (fig. 15(b)) was analyzed in a manner similar to that used in appendix A. This figure shows three  $\gamma$  spots (enclosed in circles and designated with indices in parentheses) together with the expected  $\delta$  spots (enclosed in squares). The  $002_{\gamma}$  spot was used to obtain the dark field electron micrograph of these precipitates shown in figure 15(c). This analysis suggests that these precipitates are  $\gamma$ . These precipitates may, however, be  $\gamma'$ , and the superlattice diffraction spots [(001), (110)] $\gamma'$  (ref. 2) may be too weak to be detected in the diffraction pattern. Lemkey et al. have observed  $\gamma'$  precipitates in  $\delta$  regions of the  $\gamma/\gamma' - \delta$  eutectic alloy (ref. 1). Lemkey has, however, recently observed both  $\gamma$  and  $\gamma'$  precipitates in  $\delta$  (private communication with F. D. Lemkey of United Technology Research Center). Because of the absence of superlattice diffraction points observed in this study, these fine precipitates were assumed to be  $\gamma$ .

## REFERENCES

1. Lemkey, F. D. ; and McCarthy, G. : Quarternary and Quinary Modifications of Eutectic Superalloys Strengthened by  $\delta$ ,  $\text{Ni}_3\text{Cb}$  Lamellae and  $\gamma'$ ,  $\text{Ni}_3\text{Al}$  Precipitates. (R911698-13, United Aircraft Corp. ; NAS3-17785) NASA CR-134678, 1975.
2. Lemkey, F. D. : Eutectic Superalloys Strengthened by  $\delta$   $\text{Ni}_3\text{Cb}$  Lamellae and  $\delta'$   $\text{Ni}_3\text{Al}$  Precipitates. NASA CR-2278, 1973.
3. Gray, Hugh R. ; and Sanders, William A. : Effect of Thermal Cycling in a Mach 0.3 Burner Rig on Properties and Structure of Directionally Solidified  $\gamma/\gamma' - \delta$  Eutectic. NASA TM X-3271, 1975.
4. Annarumma, P. ; and Turpin, M. : Structure and High Temperature Mechanical Behavior of Ni- $\text{Ni}_3\text{Nb}$  Unidirectional Eutectic. Met. Trans. , vol. 3, no. 1, Jan. 1972, pp. 137-145.
5. Paulonis, D. F. ; Oblak, J. M. ; and Duval, D. S. : Precipitation in Nickel-Base Alloy 718. ASM Trans. , vol. 62, no. 3, Sept. 1969, pp. 611-622.
6. Duval, D. S. ; and Donachi, M. J. , Jr. : Precipitation Characteristics of Nickel-Rich Ni-Al-Nb Alloys. J. Inst. Metals, vol. 100, 1972, pp. 6-12.
7. Kraft, E. H. ; Thompson, E. R. ; and Patarini, V. M. : Develop, Fabricate and Test High Strength Directionally Solidified Eutectic Alloys. UARL-N911649-3, United Aircraft Corp. (AD-778655), 1974.
8. Gell, M. ; and Barkalow, R. H. : Microstructure-Property Relationships of a Directionally Solidified Superalloy Eutectic. The Microstructure and Design of Alloys. Proc. Third Int. Conf. Strength of Metals and Alloys. Vol. 1, Metals Soc. (London), 1973, pp. 261-265.
9. Gell, M. ; and Donachie, M. J. : Directionally Solidified Eutectics for Use in Advanced Gas Turbine Engines. Materials on the Move: Proc. Sixth Nat. Tech. Conf. , Soc. Advancement of Mat. and Process Eng. , 1974, pp. 188-195.

TABLE I. - THERMAL TREATMENTS AND MICROSTRUCTURAL OBSERVATIONS<sup>a</sup>

| Temperature  | Thermal treatment     |                 | Microstructural observation  |  |
|--------------|-----------------------|-----------------|--|--|
|              | Aging temperature, °C | Aging time, hr  | Material condition   |  |
|              |                       | 0<br>(no aging) | As directionally solidified  | $\gamma'$ solutioned (4 hr at 1225° C, air quenched)   |
| Low          | 750                   | 16 and 48       | Cuboidal $\gamma'$ (0.4 $\mu\text{m}$ ) and disk shaped $\gamma'$ <sup>b</sup> in $\gamma$ ; occasional lath shaped $\delta$ in cellular $\gamma$            | Cuboidal $\gamma'$ (0.15 $\mu\text{m}$ ) in $\gamma$   |
|              | 800                   | 16 and 48       |  | Cuboidal $\gamma'$ (0.14 $\mu\text{m}$ ) in $\gamma$   |
|              | 850                   | 8 and 24        |  | Cuboidal $\gamma'$ (0.16 $\mu\text{m}$ ) in $\gamma$   |
| Intermediate | 900                   | 8 and 24        | $\gamma$ in $\delta$ & $\delta$ in $\gamma$ (more in cellular regions); $\gamma'$ in $\gamma$ coarsens and becomes spheroidal as aging temperature increases | Cuboidal $\gamma'$ (0.18 $\mu\text{m}$ ) in $\gamma$ and $\gamma''$ in $\gamma$  |
|              | 950                   | 8 and 24        |  | Cuboidal $\gamma'$ (0.29 $\mu\text{m}$ ) in $\gamma$ ; $\gamma''$ in $\gamma$ ; $\gamma$ in $\delta$ and $\delta$ in $\gamma$ (more in cellular regions)               |
| Elevated     | 1040                  | 8               |  | Cuboidal $\gamma'$ (0.29 and 0.38 $\mu\text{m}$ ) in $\gamma$ ; $\gamma''$ in $\gamma$ ; $\delta$ in $\gamma$ and less $\gamma$ in $\delta$ (more in cellular regions) |
|              | 1120                  | 8               |  | Spheroidal $\gamma'$ (0.48 $\mu\text{m}$ ) in $\gamma$ ; less and coarser $\gamma$ in $\delta$ ; more and coarser $\delta$ in $\gamma$                                 |
|              |                       |                 |  | Spheroidal $\gamma'$ (0.68 $\mu\text{m}$ ) in $\gamma$ ; more and coarser $\delta$ in $\gamma$ ; less and coarser $\gamma$ in $\delta$                                 |

<sup>a</sup>All had alternate lamellae of  $\gamma/\gamma'$  and  $\delta$  (less than 25 percent cellular region).

<sup>b</sup> $\gamma''$  is bct  $\text{Ni}_3\text{Nb}$ .

TABLE II. - EFFECT OF HEAT TREATMENTS ON TENSILE AND STRESS-RUPTURE PROPERTIES  
OF DIRECTIONALLY SOLIDIFIED  $\gamma/\gamma'$  -  $\delta$  EUTECTIC ALLOY<sup>a</sup>

| Solution treatment          | Aging treatment             | Tensile properties (925 <sup>o</sup> C) |                     |                            | Stress-rupture properties (870 <sup>o</sup> C and 515 MN/m <sup>2</sup> ) |                     |                            |
|-----------------------------|-----------------------------|---|---------------------|----------------------------|---|---------------------|----------------------------|
|                             |                             | Tensile strength, MN/m <sup>2</sup>     | Elongation, percent | Reduction in area, percent | Rupture life, hr  | Elongation, percent | Reduction in area, percent |
| 4 hr at 1225 <sup>o</sup> C | No aging                    | 960                                     | 5                   | 2                          | 96  | 9                   | 18                         |
|                             | 24 hr at 900 <sup>o</sup> C | 945                                     | 2                   | 3                          | 200   | 10                  | 16                         |
|                             | 8 hr at 1100 <sup>o</sup> C | 805                                     | 2                   | 5                          | 246   | 8                   | 9                          |
| 4 hr at 1210 <sup>o</sup> C | No aging                    | 930                                     | 3                   | 1                          | 119   | 9                   | 22                         |
|                             | 24 hr at 900 <sup>o</sup> C | 910                                     | 3                   | 4                          | 350   | 10                  | 14                         |
|                             | 8 hr at 1100 <sup>o</sup> C | 800                                     | 2                   | 3                          | 363   | 10                  | 15                         |
| As directionally solidified | No aging                    | 820                                     | 3                   | 5                          | 120   | 7                   | 12                         |
|                             | 24 hr at 900 <sup>o</sup> C | 855                                     | 2                   | 3                          | 293   | 7                   | 11                         |
|                             | 8 hr at 1100 <sup>o</sup> C | 895                                     | 3                   | 6                          | 304   | 6                   | 10                         |

<sup>a</sup>Growth rate, 3 cm/hr.

TABLE III. - TEMPERATURE DEPENDENCE OF STRESS-RUPTURE AND TENSILE PROPERTIES OF HEAT-TREATED<sup>a</sup> DIRECTIONALLY SOLIDIFIED  $\gamma/\gamma'$  -  $\delta$  EUTECTIC ALLOY<sup>b</sup>

| (a) Tensile properties |                                     |                     |                            |
|------------------------|-------------------------------------|---------------------|----------------------------|
| Temperature, °C        | Tensile strength, MN/m <sup>2</sup> | Elongation, percent | Reduction in area, percent |
| Room (23)              | 1400                                | 1                   | 3                          |
|                        | 1410                                | 4                   | 3                          |
| 760                    | 1115                                | 7                   | 10                         |
|                        | 1165                                | 2                   | 6                          |
| 925                    | 940                                 | 3                   | 3                          |
|                        | 1025                                | 4                   | 3                          |
| 1040                   | 655                                 | 13                  | 20                         |
|                        | 650                                 | 19                  | 21                         |

| (b) Stress-rupture properties                 |                  |                     |                            |
|---|------------------|---------------------|----------------------------|
| Temperature and stress, °C, MN/m <sup>2</sup> | Rupture life, hr | Elongation, percent | Reduction in area, percent |
| 760/760                                       | 3648.7           | 1                   | 6                          |
|   | 2182.0           | 1                   | 3                          |
| 800/690                                       | 1149.7           | 7                   | 8                          |
|   | 318.5            | 2                   | 5                          |
| 870/515                                       | 324.0            | 8                   | 8                          |
|   | 445.0            | 6                   | 8                          |
|   | 308.3            | 5                   | 9                          |
| 1040/340                                      | 3.3              | 11                  | 21                         |
|   | 4.5              | 15                  | 18                         |
| 1040/150                                      | 151.5            | 12                  | 16                         |
|   | 234.8            | 12                  | 16                         |

<sup>a</sup>4 hr/1210° C - air quenched - 24 hr/900° C - air quenched.

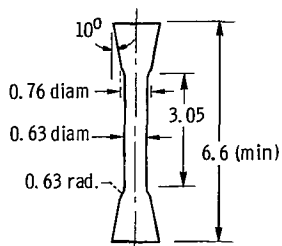
<sup>b</sup>Growth rate, 4 cm/hr.

TABLE IV. - COMPARISON OF OBSERVED<sup>d</sup> SPACINGS WITH SPACINGS CALCULATED FOR BODY CENTERED TETRAGONAL Ni<sub>3</sub>Cb( $\gamma''$ )  
[ $a_0 = 3.0 \times 10^{-10}$  m (3.624 Å),  $c_0 = 7.4 \times 10^{-10}$  m (7.406 Å).]

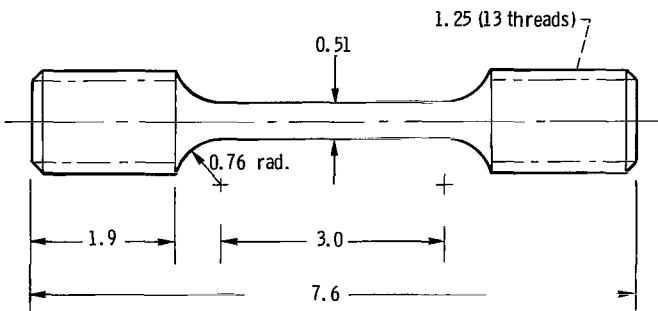
| Radii, r, cm | Observed                        | Calculated <sup>b</sup> |     |
|--------------|---------------------------------|-------------------------|-----|
|              | d spacing <sup>a</sup> = k/r, m | d spacing, m            | hkl |
| 1.25         | $3.78 \times 10^{-10}$          | $3.703 \times 10^{-10}$ | 002 |
| 1.47         | 3.21                            | 3.255                   | 101 |
| 1.84         | 2.57                            | 2.56                    | 110 |
| 2.15         | 2.20                            | 2.10                    | 112 |
| 2.28         | 2.07                            | 2.04                    | 103 |
| 2.55         | 1.85                            | 1.85                    | 004 |
| 2.7          | 1.75                            | 1.81                    | 200 |
| 3.6          | 1.31                            | 1.295                   | 204 |
| 4.3          | 1.10                            | 1.145                   | 310 |
| 4.62         | 1.02                            | 1.054                   | 224 |
| 4.88         | .96                             | .99                     | 321 |
| 5.38         | .87                             | .873                    | 411 |
| 5.54         | .85                             | .854                    | 330 |
| 5.75         | .82                             | .81                     | 420 |
| 6.5          | .72                             | .721                    | 431 |
| 6.88         | .68                             | .695                    | 433 |

<sup>a</sup>Camera constant,  $k = 4.73$ .

$$d = \sqrt{1 / \left( \frac{h^2 + k^2}{a_0^2} + \frac{l^2}{c_0^2} \right)}$$

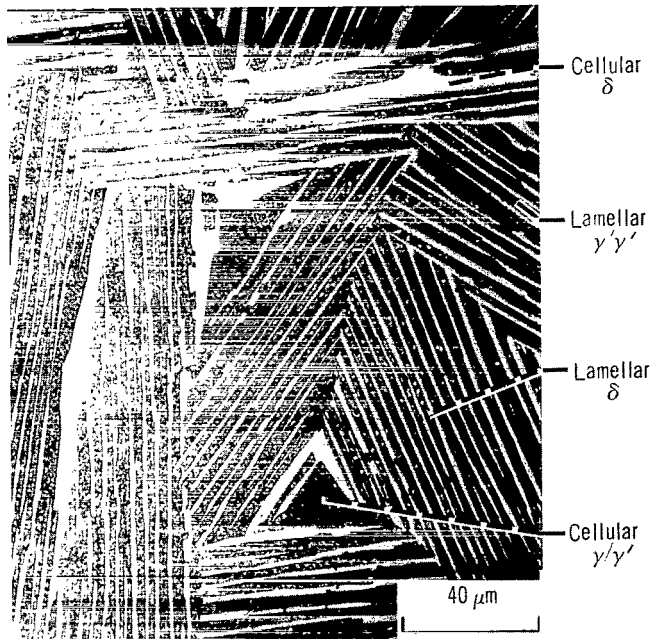


(a) Taper head specimen.



(b) Threaded head specimen.

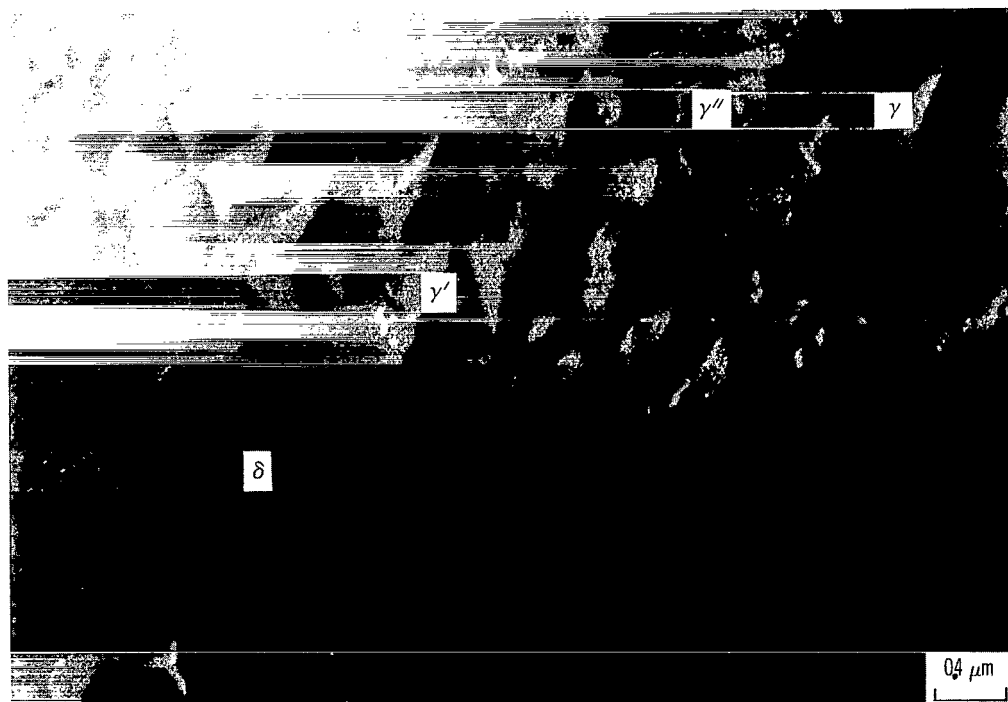
Figure 1. - Mechanical property test specimens. (Dimensions are in cm.)



(a) Light micrograph.



(b) SEM micrograph ( $\gamma/\gamma'$  matrix etched out).

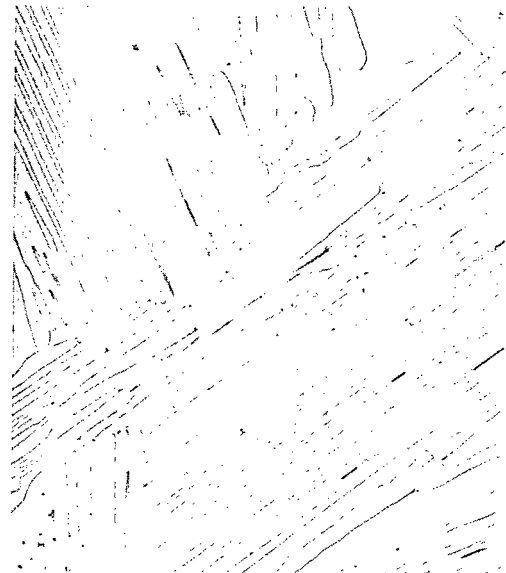


(c) Electron micrograph of ion-etched specimen.

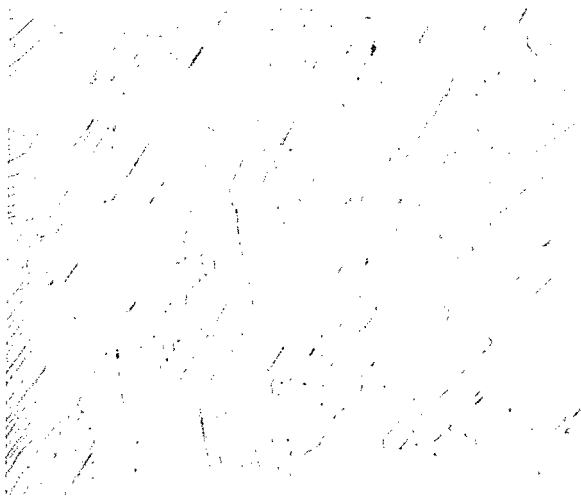
Figure 2. - Directionally solidified  $\gamma/\gamma'$ - $\delta$  eutectic alloy (transverse sections).



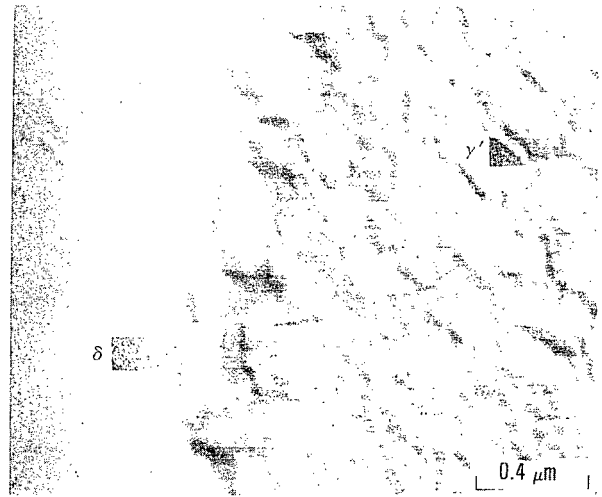
(a) Solution treatment, 4 hours at 1210° C, air quenched.



(b) Solution treatment, 4 hours at 1220° C, air quenched.



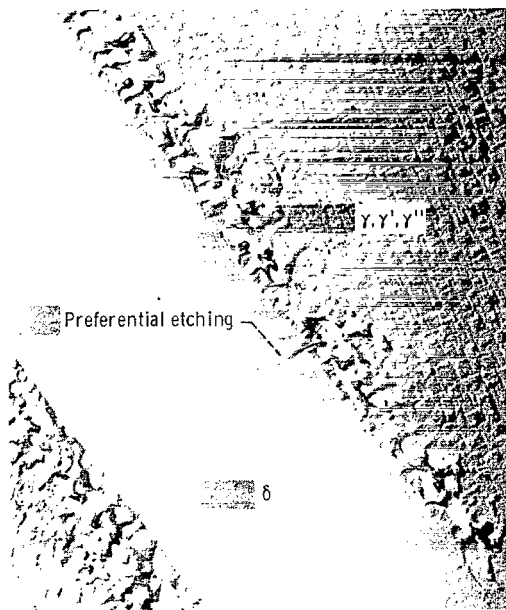
(c) Solution treatment, 4 hours at 1230° C, air quenched.



(d) Solution treatment, 4 hours at 1225° C, air quenched. (Electron micrograph of chemically etched specimen).

Figure 3. - Extent of  $\gamma'$  solutioning as function of anneal temperature. Note presence of  $\gamma'$  particles in (a) and (b) and absence in (c). (Transverse sections.)



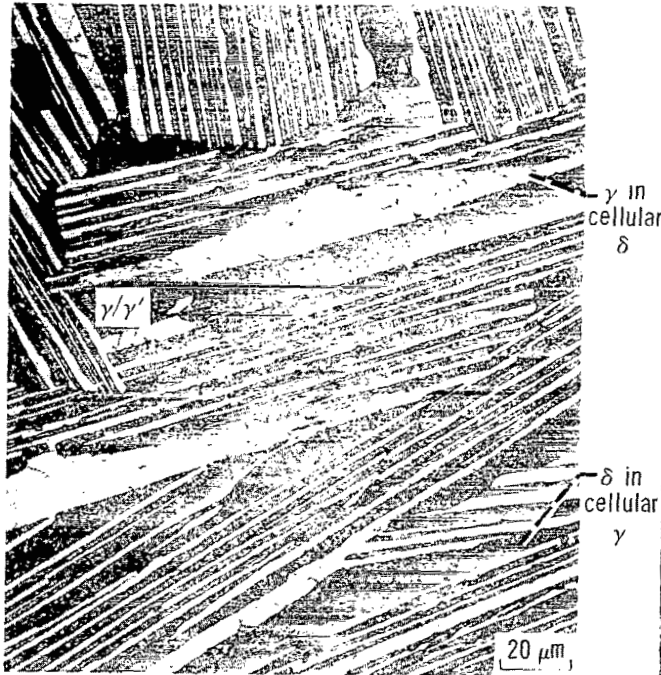


(a) Four hours at 1225<sup>o</sup> C plus 24 hours at 850<sup>o</sup> C.



(b) As directionally solidified plus 24 hours at 850<sup>o</sup> C.

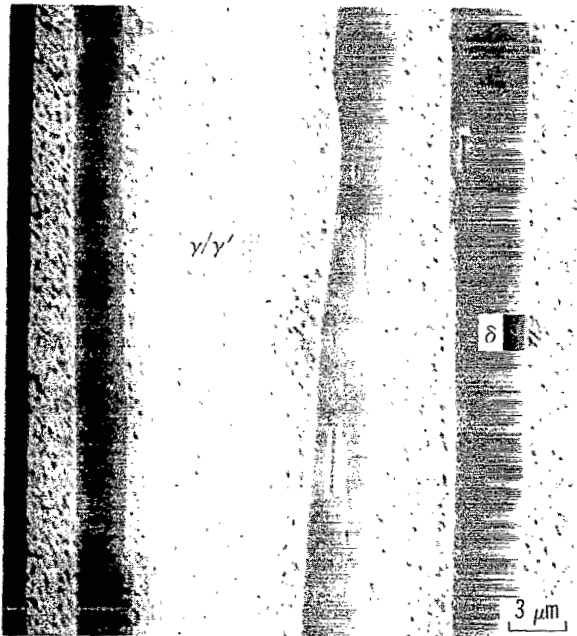
Figure 4. - Microstructure of  $\gamma/\gamma'$  -  $\delta$  eutectic alloy after low temperature aging treatment. (Electron micrographs of chemically etched specimens.)



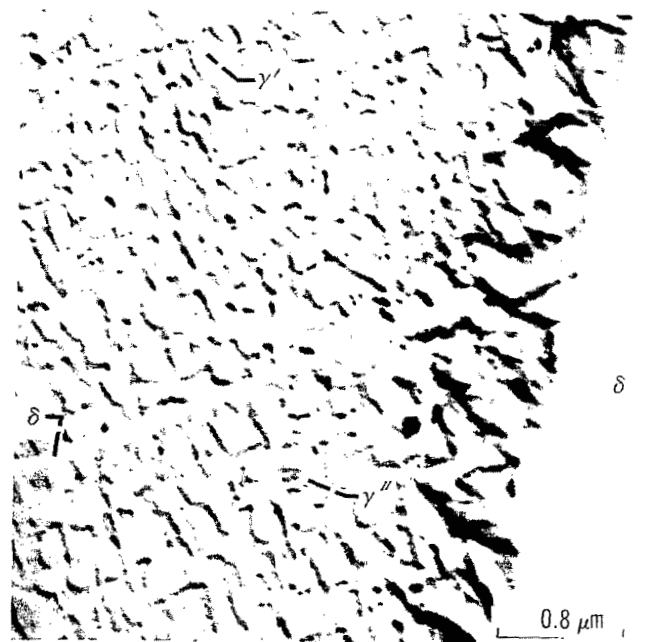
(a)  $\gamma'$  solutioned (4 hr at 1225°C) and aged. (Transverse section.)



(b)  $\gamma'$  solutioned (4 hr at 1225°C) and aged. (Transverse section, SEM micrograph.)



(c)  $\gamma'$  solutioned (4 hr at 1225°C) and aged. (Longitudinal section, SEM micrograph.)



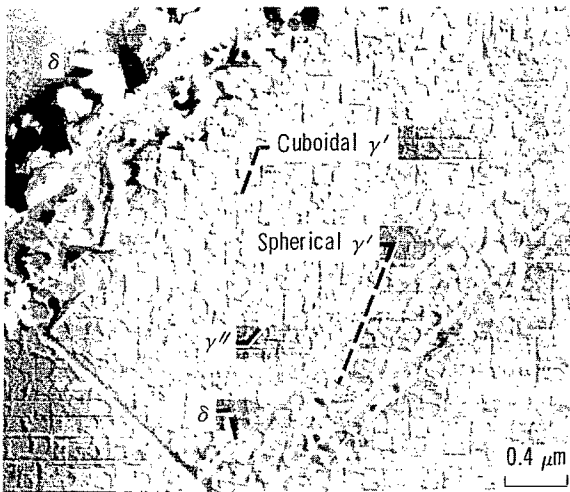
(d)  $\gamma'$  solutioned (4 hr at 1225°C) and aged. (Electron micrograph of transverse section.)

Figure 5. - Microstructural changes due to 8-hour aging at 900°C in  $\gamma/\gamma'$ - $\delta$  eutectic alloy.

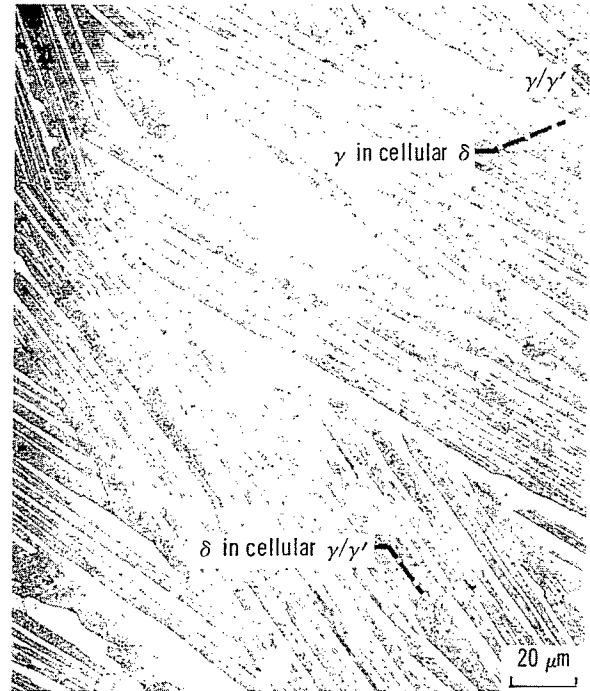


(e) Directionally solidified and aged.

Figure 5. - Concluded.

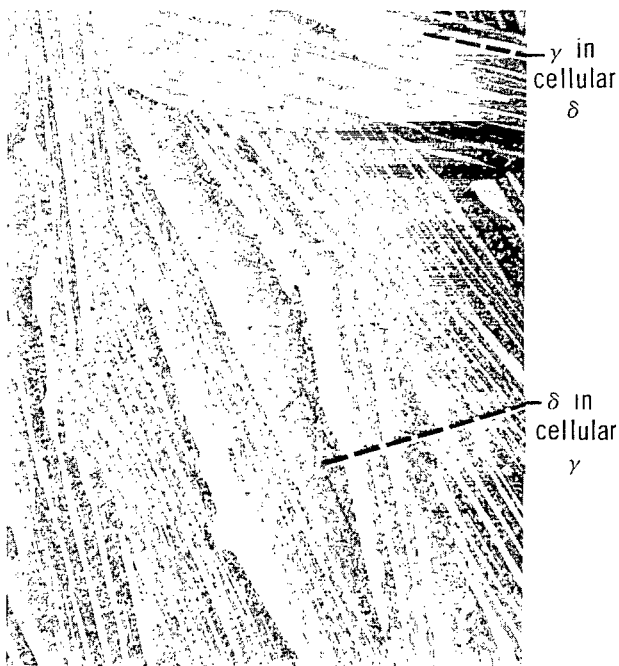


(a) Electron micrograph.

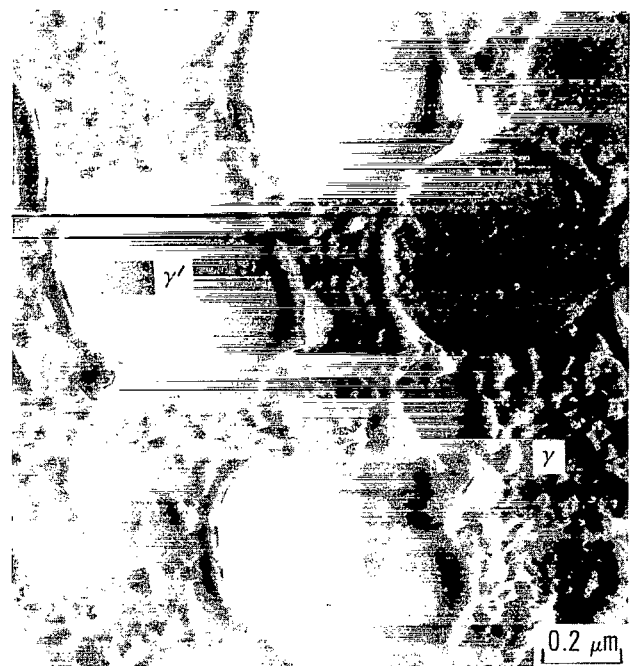


(b) Light micrograph.

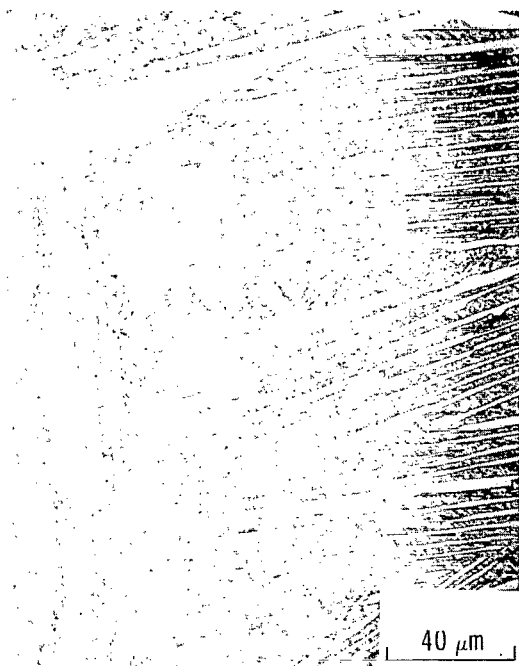
Figure 6. - Microstructure of  $\gamma'$  solutioned (4 hr at 1225°C) and aged (8 hr at 950°C)  $\gamma/\gamma'$  -  $\delta$  eutectic alloy (transverse sections).



(a) Aging, 8 hours at 1040° C.



(b) Aging, 8 hours at 1040° C (electron micrograph).



(c) Aging, 8 hours at 1120° C.



(d) Aging, 8 hours at 1120° C (electron micrograph of ion-etched surface).

Figure 7. - Effects of elevated temperature aging following  $\gamma'$  solutioning treatment (4 hr at 1225° C) of  $\gamma/\gamma' - \delta$  eutectic alloy (transverse sections).

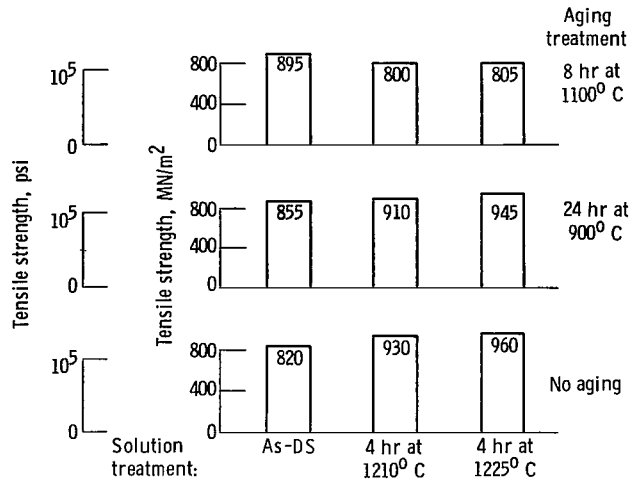


(a) Aging, 8 hours at 1100° C.

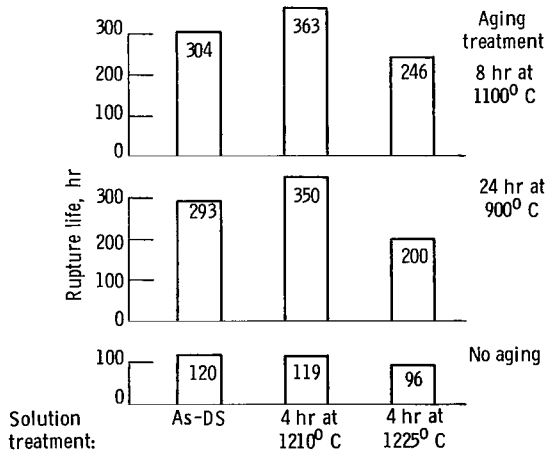


(b) Aging, 24 hours at 900° C.

Figure 8. - Effect of aging treatments following partial  $\gamma'$  solution treatments of 4 hours at 1210° C (transverse sections).



(a) Effect of heat treatment on 925° C tensile strength.



(b) Effect of heat treatment on stress rupture life. (Tests at 870° C and 515 MN/m<sup>2</sup> (75 000 psi).)

Figure 9. - Effect of heat treatment on tensile and stress-rupture properties of  $\gamma/\gamma'$  -  $\delta$  eutectic alloy.

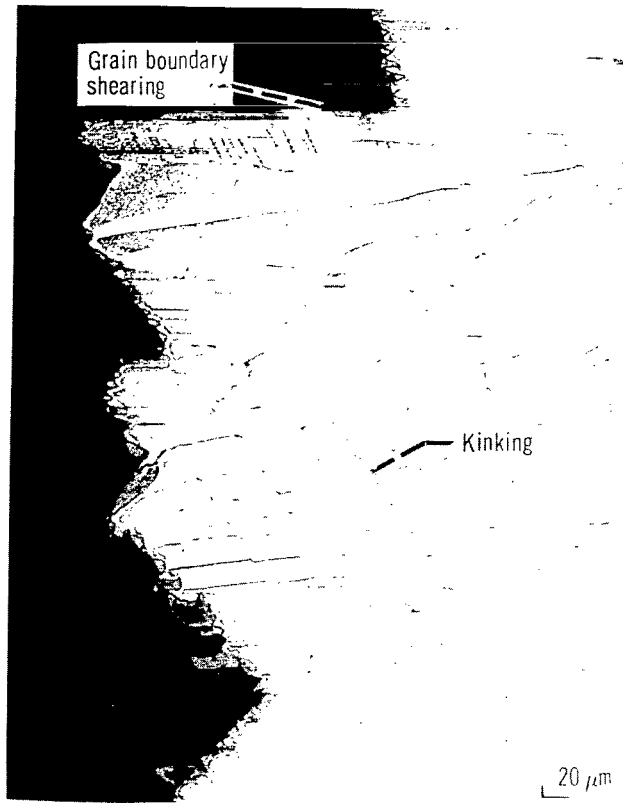


Figure 10. - Microstructural appearance of typical tensile fracture (925 °C). (Longitudinal section.)

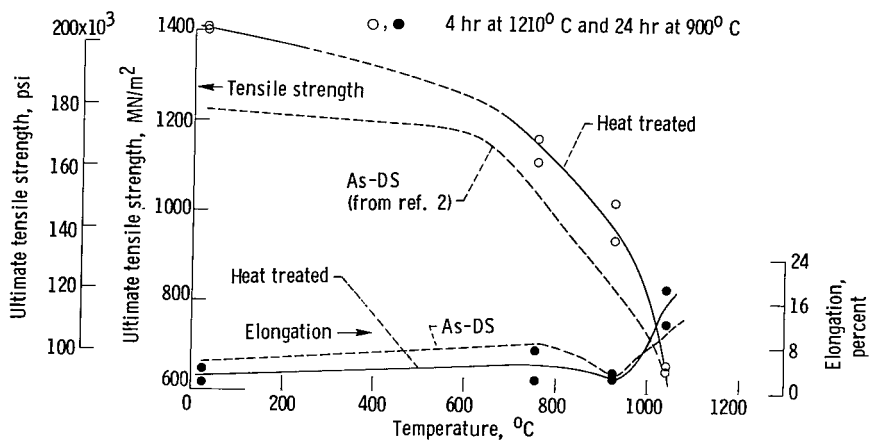


Figure 11. - Effect of temperature on tensile properties of  $\gamma/\gamma' - \delta$ .



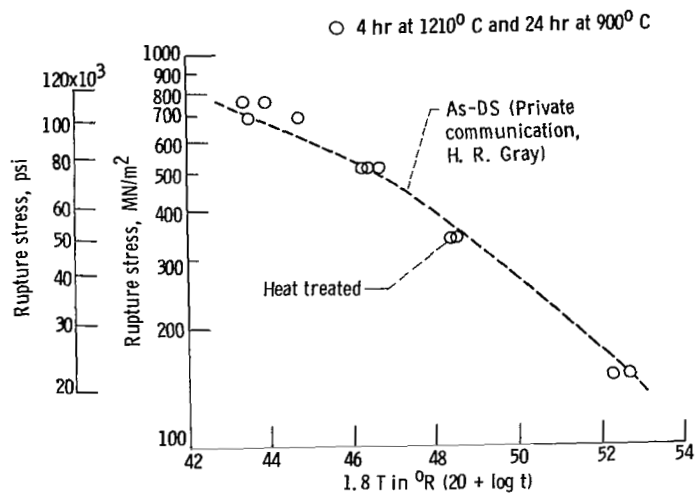
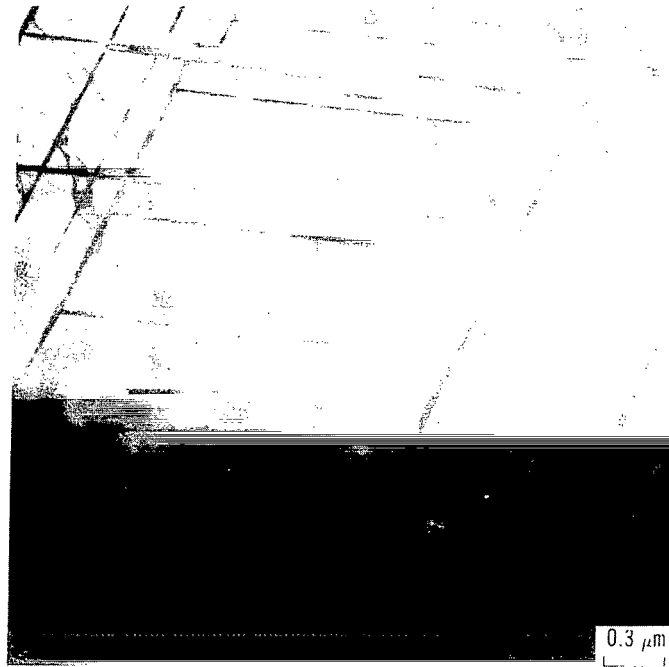
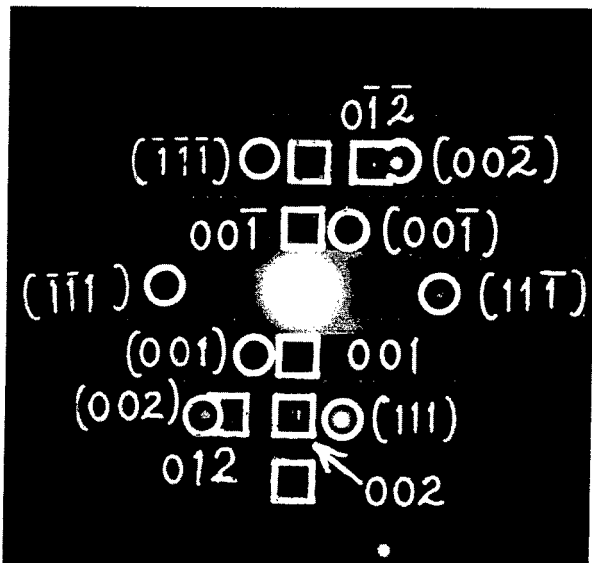


Figure 12. - Comparison of stress-rupture strength of directionally solidified and heat treated  $\gamma/\gamma' - \delta$ .



(a) Bright field electron micrograph of lath-like precipitates in  $\gamma/\gamma'$ .



(b) Electron diffraction pattern attained from  $\gamma/\gamma'$  region containing lath-like precipitates shown in (a).

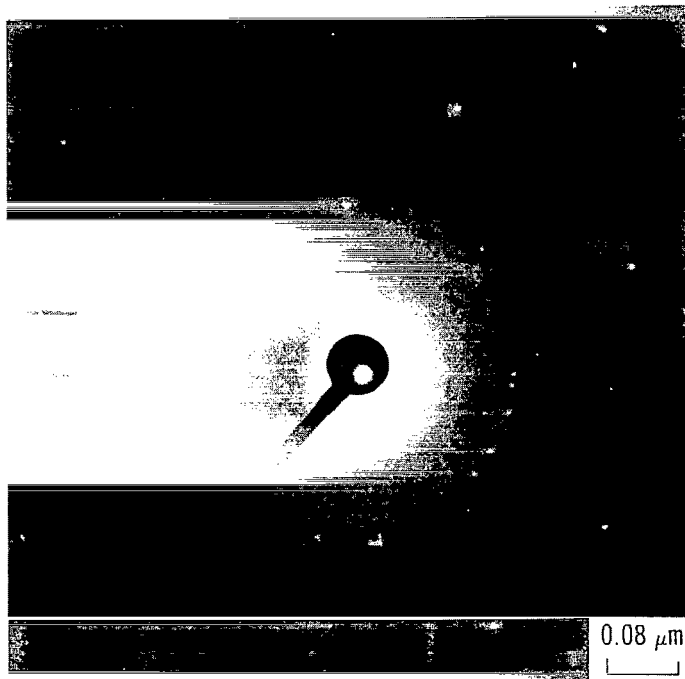


(c) Dark field electron micrograph of lath-like precipitates using  $[002] \delta$  diffraction spot shown in figure 14.

Figure 13. - Identification of lath-like precipitates observed in  $\gamma/\gamma'$  regions of directionally solidified  $\gamma/\gamma' - \delta$  eutectic alloy.



(a) Extracted  $\gamma''$  particles.

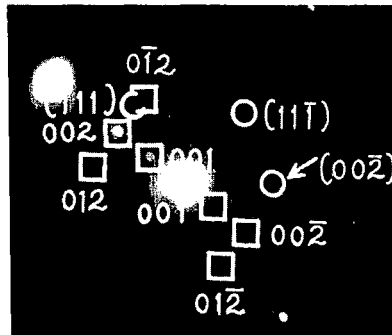


(b) Electron diffraction pattern from extracted  $\gamma''$ .

Figure 14. - Identification of extracted  $\gamma''$ .



(a) Bright field electron micrograph of fine precipitates observed in  $\delta$  regions.



(b) Electron diffraction pattern obtained from  $\delta$  region containing fine precipitates (see (a)).



(c) Dark field electron micrograph showing fine precipitates in  $\delta$  region (see (a)) using  $00\bar{2}$   $\gamma$  diffraction point shown in (b).

Figure 15. - Identification of fine precipitates observed in  $\delta$  regions of directionally solidified  $\gamma/\gamma'$  -  $\delta$  eutectic alloy after 8-hour anneal at  $900^\circ\text{C}$  following  $\gamma'$  solutioning treatment (4 hr at  $1225^\circ\text{C}$ ).



688 001 C1 U C 760806 S00903DS  
DEPT OF THE AIR FORCE  
AF WEAPONS LABORATORY  
ATTN: TECHNICAL LIBRARY (SUL)  
KIRTLAND AFB NM 87117

POSTMASTER: If Undeliverable (Section 158  
Postal Manual) Do Not Return

*"The aeronautical and space activities of the United States shall be conducted so as to contribute . . . to the expansion of human knowledge of phenomena in the atmosphere and space. The Administration shall provide for the widest practicable and appropriate dissemination of information concerning its activities and the results thereof."*

—NATIONAL AERONAUTICS AND SPACE ACT OF 1958.

## NASA SCIENTIFIC AND TECHNICAL PUBLICATIONS

**TECHNICAL REPORTS:** Scientific and technical information considered important, complete, and a lasting contribution to existing knowledge.

**TECHNICAL NOTES:** Information less broad in scope but nevertheless of importance as a contribution to existing knowledge.

**TECHNICAL MEMORANDUMS:** Information receiving limited distribution because of preliminary data, security classification, or other reasons. Also includes conference proceedings with either limited or unlimited distribution.

**CONTRACTOR REPORTS:** Scientific and technical information generated under a NASA contract or grant and considered an important contribution to existing knowledge.

**TECHNICAL TRANSLATIONS:** Information published in a foreign language considered to merit NASA distribution in English.

**SPECIAL PUBLICATIONS:** Information derived from or of value to NASA activities. Publications include final reports of major projects, monographs, data compilations, handbooks, sourcebooks, and special bibliographies.

**TECHNOLOGY UTILIZATION PUBLICATIONS:** Information on technology used by NASA that may be of particular interest in commercial and other non-aerospace applications. Publications include Tech Briefs, Technology Utilization Reports and Technology Surveys.

Details on the availability of these publications may be obtained from:

**SCIENTIFIC AND TECHNICAL INFORMATION OFFICE**

**NATIONAL AERONAUTICS AND SPACE ADMINISTRATION**

Washington, D.C. 20546